Review of SAR Measurement Methods in Relation to Wearable Devices

J. C. Wang, E. G. Lim, M. Leach, Z. Wang and K. L. Man

***Abstract*—In recent years, there has been public concern about the possibility of biological hazards from human exposure to electromagnetic radiation (EMR) emitted by wearable sensors or devices. Specific absorption rate (SAR), is used as a factor to estimate health risks and needs to be measured to meet the safety limits recommended by the IEEE/FCC. Two SAR measurement methods, namely, the Electric-field probe method and the thermographic method, are reviewed in this paper with respect to the measurement system and procedure.**

***Index Terms*—Wireless Body Area Network (WBAN), specific absorption rate (SAR), tissue-equivalent phantom, Electric-field probe method, thermographic method.**

I. Introduction

WEARABLE electronics are increasingly prevailing because of the extensive applications for wireless body area networks (WBANs), wireless sensor area networks (WSANs) and wireless local area networks (WLANs). Wireless body area networks, as body centric communication technology, have the potential to provide unprecedented opportunities for monitoring in a variety of domains, such as ubiquitous real-time healthcare and fitness, sports and military. Antennas play a pivotal role in body-centric communications and arouse significant attention in research, especially regarding possible health risks. The general performance requirements for WBAN antennas are listed in the following:

--low mutual influence between antennas and the human body for high antenna efficiency and low specific absorption rate (SAR);

--small size and low profile;

--antenna polarization is normal to the body surface, especially in on-body communications [1].

There has been increasing public concern about the possibility of biological hazards arising from human exposure to electromagnetic radiation (EMR) emitted by wearable sensors or devices in response to their increased usage over recent years. The current basic safety limits applicable to the wireless device are defined in terms of specific absorption rate (SAR), which is defined as the rate at which a person absorbs Electromagnetic energy per unit mass; where SAR averaged over X grams of tissue can be denoted by X-g SAR. The SAR in a biological body exposed to a radio frequency (RF) field depends on a number of factors, including tissue geometry and dielectric properties and the orientation of the body relative to the source [2]. There exist three different limits defined by: 1) a whole-body average SAR; 2) a local peak SAR; and 3) a specific absorption (SA), which limits the power of short pulses. 1) and 2) must be averaged over a defined period of time. In wireless devices at frequencies above 300 MHz, the absorption affects only parts of the body, which are close to the device. Hence, the most critical value is the local peak SAR limit. Localized SAR averaged over 10-g and 1g of tissue i.e. peak 10-g SAR and peak 1-g SAR not exceeding 2.0 W/kg and 1.6 W/kg respectively, are recommended by the IEEE/ANSI/FCC as the upper safety limit [3].

Evaluating the SAR distributions associated with electronic devices is a complex task, usually accomplished by measurement techniques or numerical modeling. Two experimental methods to evaluate compliance with specific SAR requirements use measurement of either, the electric field (E-field) strength or, the rate of temperature increase in a tissue-equivalent liquid using anthropomorphic models of the human head or other part. This paper is an extended version of [4]. In this paper, evaluation of SAR distributions by E-field probe and by thermographic measurement is reviewed. Also applications of these two methods are presented in section IV.

II. The Common Phantom

Electronic devices or antennas resulting in microwave radiation exposure to humans require safety limits to avoid potential health hazards. In order to evaluate the near-field exposure produced by wireless on-body devices, phantom models simulating the human body are used. There are some common phantoms adopted for SAR measurements.

A. The Averaged Tissue-equivalent Liquid Phantom

An averaged tissue-equivalent liquid phantom is required in order to simulate the human body dielectric environment when measuring antennas or estimating SAR values near the human body. This phantom is commonly a mixture of sugar, Sodium Chloride, De-ionized water, Hydroxyethyl Cellulose, Bactericide, Diethylene Glycol Butyl Ether, Triton X-100,

Manuscript received July 30, 2016. This work is partially supported by the Natural Science Foundation of Jiangsu province (No. BK20131183) and XJTLU Research Development Fund (RDF-14-03-24 and RDF-14-02-48).

J. C. Wang is with the Jiaotong-Liverpool University, China. Email: Jingchen.Wang@xjtlu.edu.cn

E. G. Lim is with the Xi'an Jiaotong-Liverpool University, China. Email: enggee.lim@xjtlu.edu.cn

M. Leach is with the Jiaotong-Liverpool University, China. Email: mark.leach@xjtlu.edu.cn

Z. Wang is with the Xi'an Jiaotong-Liverpool University, China. Email: zhao.wang@xjtlu.edu.cn

K. L. Man is with the Xi'an Jiaotong-Liverpool University, China. Email: ka.man@xjtlu.edu.cn

Diacetin, 1,2-Propanediol [5].

When an averaged tissue-equivalent liquid phantom is used to estimate an SAR distribution, the dielectric properties of the phantom need to be checked to ensure agreement with the required conductivity and dielectric constant. The method involved in using an open-ended coaxial probe to measure liquid dielectric properties is presented in [6-7]. In using the open-ended coaxial method to measure the dielectric properties of the phantom, the error value between the phantom and realistic human tissue can be minimized, to provide an accurate SAR evaluation over the human-body phantom.

B. *The Brain-equivalent Phantom*

The composition of the brain-equivalent phantom in accordance with the COST244 as an example is deionized water, agar, sodium chloride, sodium azide TX-151 and polyethylene power [8]. The agar is utilized for maintaining the shape of the phantom by itself. The relative permittivity is controlled with additional rate of polyethylene powder. In order to mix water with the polyethylene, the TX-151 is selected for stickiness. Owing to the stickiness, both sides of the surfaces of the split phantom cling to each other. The sodium azide is a preservative. In addition, the loss factor is dependent on the concentration of the sodium chloride.

C. *The Skull-equivalent Phantom*

The recipe of the skull-equivalent solid phantom is silicone emulsion, agar, glycerol, TX-151 and polyethylene powder; the glycerol is used as a solvent. Skull tissue is a low-loss media, therefore, the solvent should be low loss and of the hydrophilic type. However, because the relative permittivity is too small only using glycerol, silicone emulsion is added [9].

The dielectric properties of a human body vary with frequency; detailed dielectric constants for human tissues are available in [10]. Therefore, the proportions of ingredients required to formulate the equivalent phantom depend on the operating frequency at which an antenna or a wireless device works. This phantom can be used in the measurement of on-body or in body electronics. The brain-equivalent phantom has the merit of ease to control the relative permittivity and conductivity by modifying the quantity of the polyethylene powder and sodium chloride. The electric constant can be controlled by changing the mixture of the glycerol and silicone emulsion concerning the skull-equivalent phantom [11]. For mobile phones or other devices used in close proximity to the brain, the brain-equivalent and skull-equivalent phantoms are proper to conduct SAR measurements. It is essential to optimize the phantom based on the operating frequency and application in order to obtain valid results.

III. EXPERIMENTAL METHODS FOR SAR MEASUREMENT

Two methods are currently available for SAR measurements, used to estimate the SAR in the human models exposed to microwave sources, these are the Electric-field probe method and the thermographic method.

A. *The Electric-field Probe Method*

The electric-field probe method, as a rapid and non - invasive SAR measurement solution, is based on utilizing automatic positioning systems to move an E-Field measuring probe in a liquid phantom to assess SAR values [12].

Experimental Theory

The specific absorption rate (SAR) is usually used as the primary dosimetric parameter of EM wave exposure for standardization [13], expressed as:

$$\mathrm{SAR}=\frac{\sigma|\mathrm{E}|^2}{\rho} \qquad [W/kg] \tag{1}$$

Where, σ[S/m] is the conductivity of the tissue, ρ [kg/m3] is the density of the tissue, and E [V/m] is the electric field intensity within the tissue.

Measurement System (DSAY-5)

Due to the FCC adopted limits for safe exposure to radiofrequency (RF) energy where the limits are defined in terms of SAR. DSAY-5 [14] (as shown in Fig.1), is the latest SAR fully automated test system. It has the capability to provide faster and more accurate SAR test and measurement than previously available test systems.

Fig. 1: The schematic of DASY-5

Measurement Setup

The system of DASY-5 consists of a PC, data acquisition Unit (DAE), E-field probe, robot controller, phantom shell with tissue, equipment under test (EUT) and device holder, as shown in Fig 2.

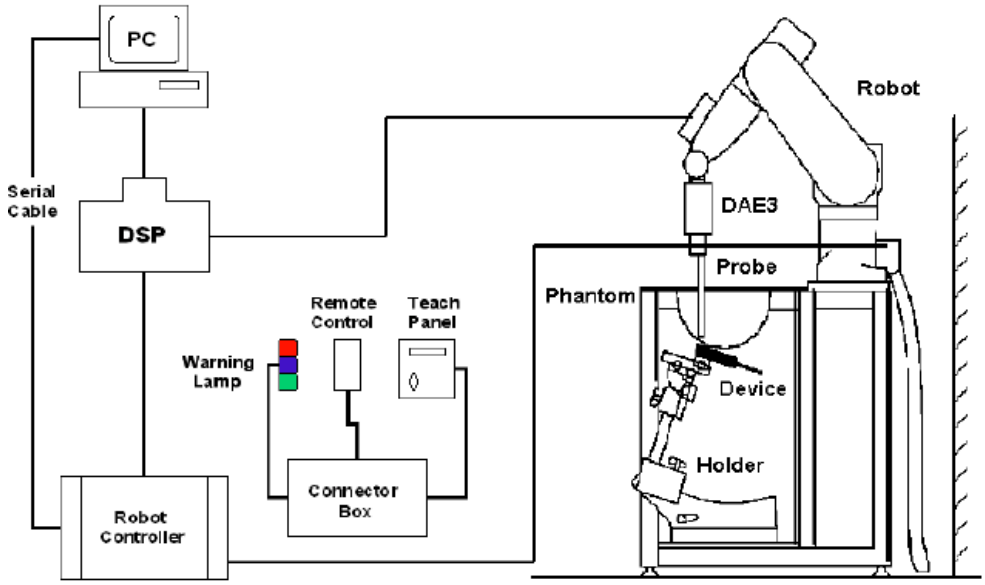

Fig. 2: The structure of SAR measurement system by using DASY-5

The SAR measurement setup [15] is shown in Fig.3.

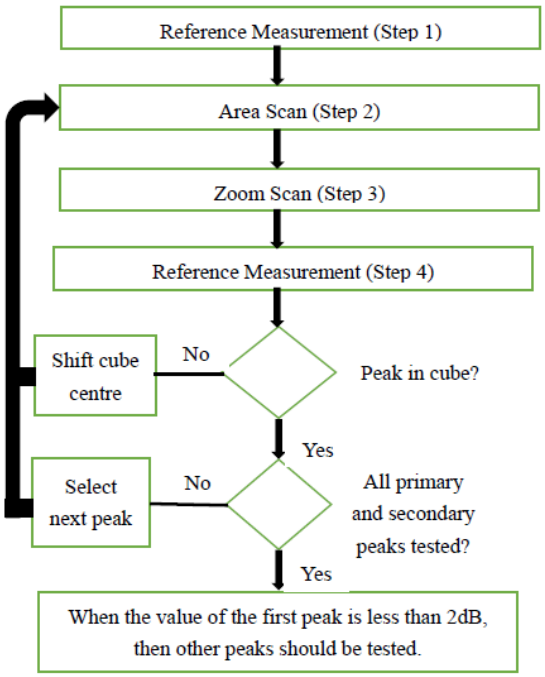

Fig. 3: The flow chart of SAR measurement setup

Firstly, is the SAR reference measurement. Prior to the SAR test, local SAR shall be measured at a stationary reference point where the SAR exceeds the lower detection limit of the measurement system. Alternatively, the conducted power may be measured if the drift assessment from SAR measurements is not sensitive enough.

Secondly, is the Area scan. The area scan aims to determine peak SAR locations. An E-field probe moves through the tissue-equivalent liquid in a SAM or a flat phantom to find approximate location(s) of SAR peak(s). The distance between phantom and probe should be more than half the probe diameter, otherwise, an increased measurement uncertainty occurs. The measured values are interpolated to identify peak locations. Typically, the local peak SAR values occur at the surface of homogeneous phantoms, which are not directly measurable by the field sensors that are located 0.5 mm to 4 mm behind the probe tip.

Thirdly, is the Zoom scan. The goal of the zoom scan is to determine cube averaged SAR. Zoom scans surrounding one or more of these peak locations are subsequently executed to determine the peak spatial-average SAR value. When the frequency is lower than 3 GHz, it uses 5×5×7 points in a 3×3×3 cm^3 cube. When the frequency is between 3 GHz and 6 GHz, then more than 7×7×7 points should be adopted. 1-g SAR is computed by extrapolating measured values to the phantom surface. After the zoom-scan measurement, extrapolations from the closest measured points to the surface, along lines parallel to the zoom-scan centerline, and interpolations to a finer resolution between all measured and extrapolated points are performed.

Finally, is the SAR drift measurement. The local SAR (or conducted power) is measured at exactly the same location as in Step 1. The absolute value of the measurement drift (the difference between the SAR measured in Step 4 and Step 1) is then recorded and the drift should be maintained within ± 5% for accuracy to be sufficient. SAR drift measurements are made after each zoom scan to assess accuracy continuing accuracy, with drift always compared to the initial measurement.

B. The Thermographic Method

The thermographic method offers a more efficiency route to establishing SAR over a two-dimensional internal plane within an exposed model. This method is described specifically in [16-17], and is valid for both far- and near-zone fields. It involves the use of a thermographic camera to record temperature distributions produced by energy absorption in phantom models after exposure to radiating fields. The model is first disassembled along a plane where SAR is to be determined and a thermograph-temperature scan is made over the plane. The model is then reassembled and exposed to a high power density signal for a short time; followed by disassembly and

another thermographic scan.

Experimental Theory

Thermographic experiments [18-19] are carried out using the brain and skull-equivalent solid phantom models to estimate the SAR distribution in human heads. If heat diffusion is negligibly small during the exposure period, the SAR at an arbitrary point is given by

$$\mathrm{SAR}=c\frac{\Delta T}{\Delta t}\quad [W/kg] \tag{2}$$

where, c [J/kg·K] is the specific heat of the phantom, ΔT [K] is the temperature rise at the point, and Δt [second] is the exposure time. Hence, the temperature rise profile is proportional to the SAR distribution on the above assumption. The specific heat of the brain and skull-equivalent phantom are 3750 and 2850 J/kg·K, respectively. This equation describes that the SAR distribution is proportional to the temperature rise.

Measurement System

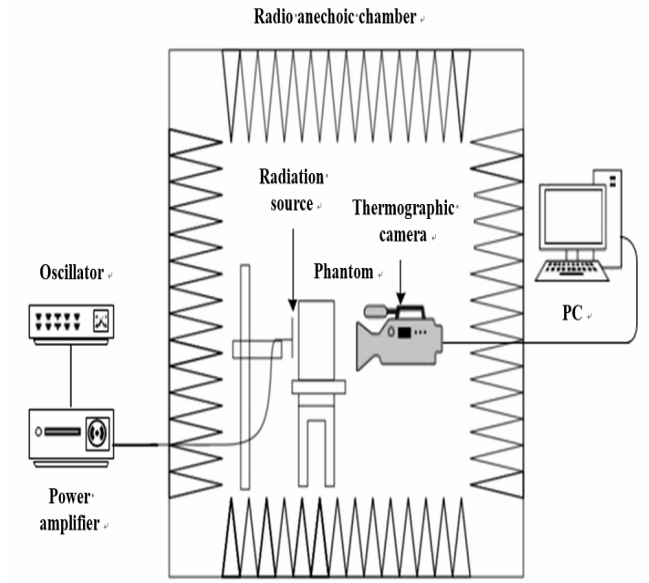

Fig. 4: SAR measurement system

The components of the thermographic SAR measurement system are a thermographic camera, a phantom, an antenna, radio anechoic chamber, oscillator, power amplifier and a computer, as shown in Fig.4.

Measurement Procedure

The measurement procedure [20] is shown in Fig.5. At first, a phantom with uniform temperature is placed in a radio anechoic chamber and exposed to UHF radio waves by a nearby source for 2 minutes or so. The exposure duration is determined to yield a temperature rise of at least 1 K. The phantom is split to observe the inside before the exposure. After the exposure period, the phantom is reopened quickly in front of a thermographic camera. A thermographic image is immediately captured to map the temperature rise profile on a section or a surface of the phantom.

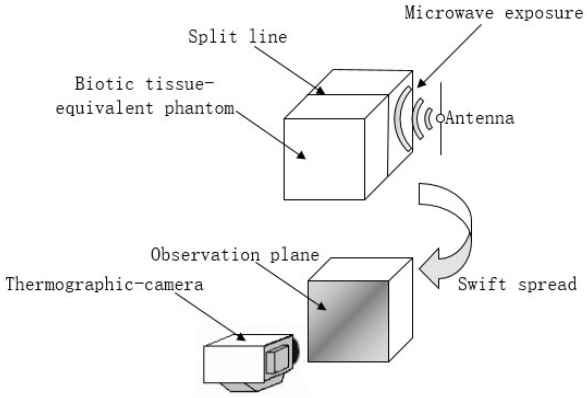

Fig. 5: SAR measurement procedure

Generally, SAR measurements in the neighborhood of the phantom boundary are difficult using the E-field probe method, though they are possible using the thermographic method as described. The use of a solid phantom in the thermographic method offers the advantage of being able to measure SAR in mediums with complicated shapes.

Some disadvantages of the thermographic method include: an inability to test real mobile telecommunication devices, due to the high power necessary for the experiment; SAR images are limited to two-dimensional cuts [11]. Therefore, the thermographic method is not suitable for the testing of real RF devices.

IV. Applications of two SAR measurement methods

A. Textile Antenna of SAR Measurement with the Electric-field Probe Method

A simple slit is adapted for the planar inverter F antenna (PIFA), which can be made from three different conductive materials, CT, SH or PCPTF [21]. This PIFA with a slit (SPIFA) operates at a center frequency of 2.45 GHz, with broad BWs between 800 MHz and 1 GHz in free space. Fig. 6 shows the broadband SPIFA prototype with an overall antenna size of 50 × 19 mm^2.

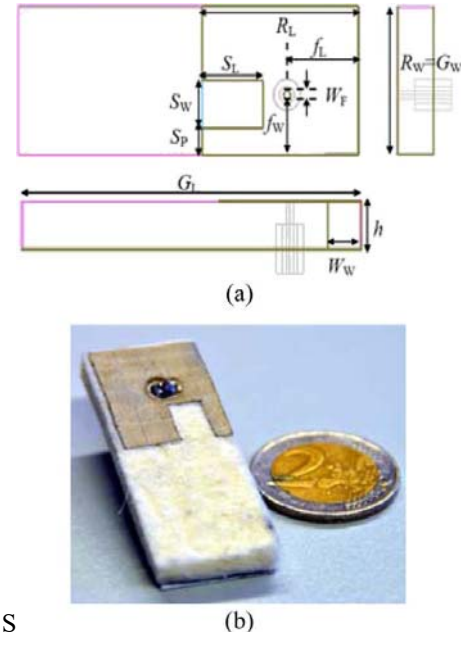

S

Fig. 6: Broadband SPIFA prototype. (a) Schematic. (b) Fabricated.

The second PIFA topology features a fractal slot on the radiator to introduce a dual-band behavior (2.45 and 5.2 GHz). This dual-band antenna features footprint sizes of 34×44 mm^2 (as shown in Fig. 7). Two types of this antenna are investigated, with one made using CT, the other made using SH, which are referred to as fractal FPIFA CT and FPIFA SH.

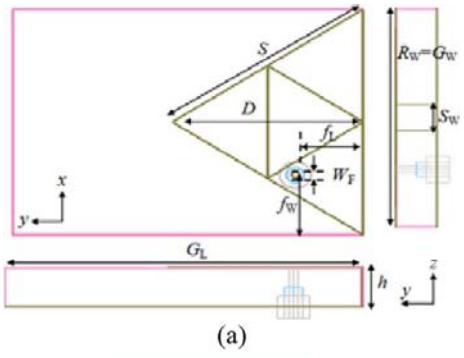

(a)

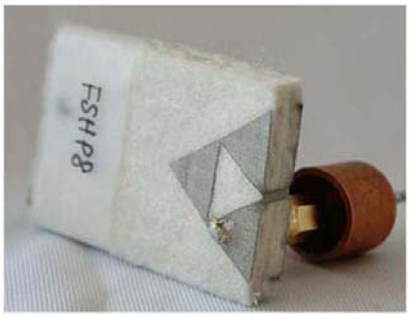

(b)

Fig. 7: Dual-band FPIFA prototype. (a) Schematic. (b) Fabricated.

To understand the SAR behavior, simulations were performed for the SPIFA and FPIFA made from the three distinct materials (two in the case of FPIFA) (see Table 1). Simulations were performed with these antennas placed both horizontally and vertically on a Hugo body model in CST. A commercial DASY-4 system from Schmid & Partners Engineering AG (SPEAG) was utilized to perform the measurements.

TABLE I: SUMMARY OF THE SIMULATED AND MEASURED SAR

Antenna Type/SAR	Freq. (GHz)	Sim. SAR (Hori.) (W/kg)	Sim. SAR (Vert.) (W/kg)	Meas. SAR (W/kg)	Diff (%) (Ave Sim vs. Meas.)
SPIFA CT	2.45	0.50	0.59	0.55	0.2
SPIFA SH	2.45	0.49	0.59	0.57	5.6
SPIFA PC	2.45	0.49	0.59	0.52	3.7
FPIFA CT	2.45	0.42	0.31	0.35	4.1
	5.20	0.63	0.57	0.50	16.7
FPIFA SH	2.45	0.39	0.28	0.30	10.5
	5.20	0.7	0.58	0.65	1.6

In Table I, the differences between the simulations and the measurements for the SPIFA prototype are small, i.e., less than 6%. However, the worst simulation–measurement difference is for the FPIFAP1 CT with about 17% at 5.2 GHz. This can be attributed to the smaller wavelength at the higher frequencies. Since it is more difficult for the flexible textile antennas to be mechanically consistent (in terms of the distance and the position) during measurements, smaller distance changes are capable of altering the location of the point of the maximum measured SAR by the probe, consequently affecting the final averaged SAR. On the contrary, the placement of the antenna at a certain distance from the numerical body model can be very accurately performed in simulations in ideal conditions, i.e., without the influence of cables, temperature, humidity, etc. Nonetheless, this should not be a cause for concern as this difference is within the published uncertainty of the measurement system [21].

B. Textile Antenna of SAR Measurement with the Thermographic Method

The RF coil employed in this paper is a birdcage coil for a 3.0 T magnetic resonance imaging (MRI) system, which operates at approximately 128 MHz [22]. This coil consists of two end rings and 16 legs, whose width are 15 and 10 mm, respectively. The diameter and length of the coil are 300 and 330 mm each, which is sufficiently large for the head model to be set inside. Additionally, the coil is enclosed in a cylindrical RF shield. The diameter and length of the RF shield are 400 and 440 mm, respectively. All these are composed of metallic sheets. Fig. 8 shows the overall and sectional views of the birdcage coil.

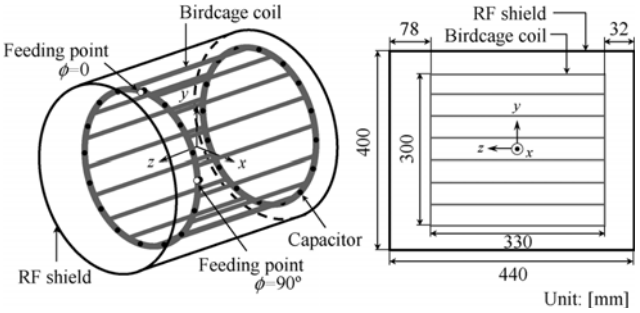

Fig. 8: Structure of birdcage coil.

The head model used in the experiment is shown in Fig. 9. This cylindrical biological tissue-equivalent solid phantom is 180 mm in diameter, 250 mm in length, and is made of a uniform medium of brain tissue. It is speculated that a cylindrical shape is suited for investigating the SAR distributions during the measurement, and in addition, it simulates the human head and neck, which are also inserted into the birdcage coil during the imaging. As compared to liquid and gel phantoms, which have to be in the case, a solid phantom is more durable and can be molded into any shape without a case.

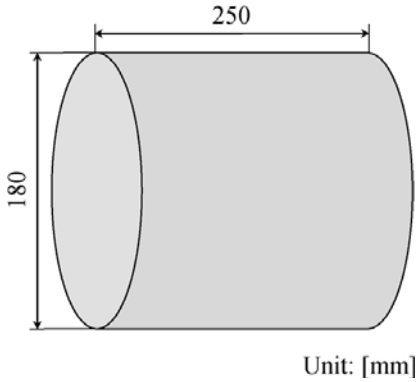

Fig. 9: Head model

Fig. 10 shows the numerical calculation model consisting of the birdcage coil and head model used to evaluate the SAR distribution. The head model shown in Fig. 9 is placed in the center of the coil.

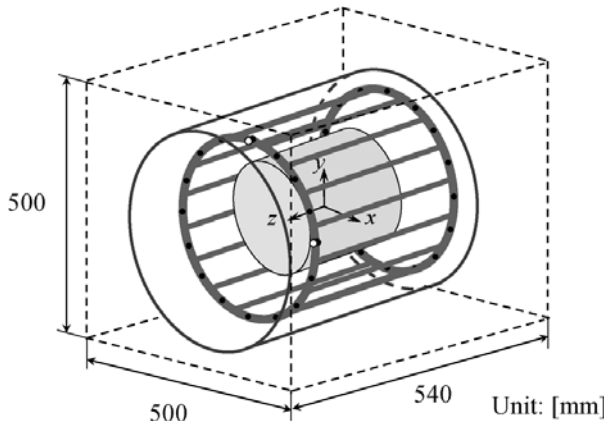

Fig. 10: Numerical calculation model.

The measurement method is via thermographic measurements. The thermographic camera used for the measurement was a TVS-200 by NEC Avio Infrared Technologies Corporation Ltd.,Tokyo, Japan, together with a power meter by Rohde & Schwarz, NRT, NAP-Z4, Munich, Germany. The exposure time was determined to achieve at least 1 K of temperature rise. In addition, the incident power was 100 W. Owing to the temperature diffusion caused by the thermal conductivity of the phantom and which cannot be neglected in this case, correction for temperature diffusion much be performed to obtain an accurate SAR value. An approximate curve was computed from the temperature transition values using equation (3):

$$f(t) = a - ae^{-bt} \tag{3}$$

where t is the exposure time, a and b are constant values.

After calculating the amount of a and b from the measured temperature rise up to 60 s, a line for the slope $f'(0)$, which can be used to neglect the temperature diffusion, was obtained. Temperature transition of the peak position is shown in Fig. 11. The correction coefficient given by (4) was used to multiply by each measured SAR value.

$$A = f'(0) \times 360s / \Delta T_m \tag{4}$$

Here, $f'(0) \times 360s$ is the temperature rise after the correction and ΔT_m is the temperature rise obtained in the measurement. The corrections for the SAR values at the observation points are listed in Table II.

TABLE II: CORRECTION OF SAR VALUE BY MULTIPLYING CORRECTION COEFFICIENT A WITH MEASURED SAR VALUES

	Before correction (W/kg)	A	After correction (W/kg)	Calculated SAR value (W/kg)
0 mm	0.31	1.29	0.40	0.42
20 mm	0.25	1.21	0.30	0.32
40 mm	0.14	1.26	0.18	0.19

From Table II, the measured SAR values get closer to the calculated results at every observation point by using the proposed correction method, and furthermore, the difference observed in the peak position decreases from 26% to 5%. The correction coefficient for the point at 20 mm inside the phantom is lower than that for the 0 mm point. This is because the inner position is influenced less by the convective effect of ambient air, which also causes a temperature decrease, especially in the surface of the phantom. Moreover, the correction coefficient for the point at 40 mm inside was greater compared to the point at 20 mm inside because the EM energy did not reach deep enough into the phantom, and hence, prevented a sufficient temperature rise for the use of the thermographic method.

V. Conclusion

Advancements in hi-technology are taking place at an accelerated rate in the present-day. Electronic apparatuses are continuously emerging on the market, from on-body devices to in-body devices for applications ranging from health to entertainment. Also, people are showing an increasing concern about the health risks associated with the use of such wearable and implanted devices. As a consequence, the measurement of SAR distributions and quantification of the effects of these devices on human tissues is of increasing importance. Results from such investigations should feed into device design considerations for example of the antenna.

Two measurement methods are currently available for conducting SAR analysis; one is the Electric-field probe method, the other is the thermographic method. The current state of the art Electric-field probe facility is the DSAY-5, however this is time consuming and expensive. The thermographic method on the other hand requires more components but it is relatively cost-efficient. However, the thermographic method is not suitable for the testing of real RF devices, though it is more adaptable for the measurement of complex shape phantoms such as inner ears and earlobes.

These two methods for SAR measurement have their own advantages and disadvantages and the most appropriate method can be selected dependent on individual measurement requirements. In future research, the deviation and accuracy of these two methods will be compared.

References

[1] P. S. Hall and Y. Hao, Antennas and Propagation for Body-Centric
Wireless Communications. Norwood, MA: Artech House, 2006.

[2] Chou, C. K., et al., “Radio frequency electromagnetic exposure: Tutorial review on experimental dosimetry,” Bioelectromagnetics, Vol. 17, pp. 195–206, 1996.

[3] Md Shaad Mahmud, Fawwaz Jinan Jibrael Jabri andBushra Mahjabeen, “Compact UWB Wearable Antenna on Leather Material for Wireless Applications”, Antennas and Propagation Society International Symposium, pp. 2191-2192,2013

[4] J. C. Wang, E. G. Lim, M. Leach, Z. Wang, K. L. Man, and Y. Huang, "Two Methods of SAR Measurement for Wearable Electronic Devices," Lecture Notes in Engineering and Computer Science: Proceedings of The International MultiConference of Engineers and Computer Scientists 2016, 16-18 March, 2016, Hong Kong, pp647-650

[5] MORLAB Offer "Tissue-simulating liquid" Products for OTA and SAR Test. 2009. http://www.morlab.cn/en/2009/0123/article_27.html.
[6] E. G. Lim, J. C. Wang, Z. Wang, T. Tillo and K. L. Man, "The UHF Band In-body Antennas for Wireless Capsule Endoscopy", Engineering Letters, vol. 21, no. 2, pp. 72-80, 2013
[7] Y. Gao, G. S. Yang, H. Wang, J. Q. Wang, S. P. Chen. "Measurement
and Amendment of Complex-permitivities of Distilled Water and Nacl Solution". J Biomed Eng. 2005, 22(3), pp. 548-549.
[8] "Proposal for numerical canonical models in mobile communications," in Proc. COST244, Rome, Italy, Nov. 1994, pp. 1–7.
[9] H. C. Taylor and J.W. Hand, "Solution of canonical problems using the
finite-difference time-domain method," in Proc. COST244, Rome, Italy, Nov. 1994, pp. 87–89
[10] Choi Y.S., Hong H.K., Kim B.J., Kim M.N., Park H.D. "Development of a Non-invasive System to measure the thickness of the subcutaneous adipose tissue layer", March 2008
[11] Y. Okano, K. Ito, I. Ida, and M. Takahashi, "The SAR evaluation method by a combination of thermographic experiments and biological tissue-equivalent phantoms," IEEE Trans. Microw. Theory Tech., vol. 48, no. 11, pp. 2094–2103, Nov. 2000
[12] Merckel. O., Gilles. Fleury, G. and Bolomey, J.-C., "Propagation model choice for rapid SAR measurement", Signal Processing Conference, 2002, pp. 1-4
[13] IEEE Standard for Safety Levels with Respect to Human Exposure to Radio Frequency Electromagnetic Fields, 3 kHz to 30 GHz, 1999
[14] SPEAG provides all components and procedures of the DASY-5 systems to meet the needs of various applications with SAR limits. . http://www.speag.com/products/dasy/dasy-systems/dasy52-sar/
[15] IEEE Recommended Practice for Determining the Peak Spatial-Average Specific Absorption Rate (SAR) in the Human Head from Wireless Communications Devices: Measurement Techniques, 2013
[16] A. W. Guy, "Analysis of electromagnetic fields induced in biological tissues by thermographic studies cmequivalent phantom models,"
IEEE Trans. Microwave Theory Tech., vol. MTT-19, pp. 205-214,
Feb. 1971
[17] M. D. Webb, A. W. Guy, and J. A. McDougafl, "Assessment of EM-field coupling of 915-MHz oven-door leakage to human subjects by thermographic studies on phantom models," J. Microwaue Power, vol. 11, pp. 162-164, 1976.
[18] Q. Balzano, O. Garay, and F. Steel, "Energy deposition in simulated human operators of 800-MHz portable transmitters," IEEE. Trans. Veh. Technol., vol. VT-27, pp. 174–181, May 1978.
[19] A.W. Guy and C.-K. Chou, "Specific absorption rates of energy in man models exposed to cellular UHF mobile-antenna fields," IEEE Trans. Microwave Theory Tech., vol. MTT-34, pp. 671–680, June 1986.
[20] T. Kobayashi, T. Nojima, K. Yamada, and S. Uebayashi, "Dry phantom composed of ceramics and its application to SAR estimation," IEEE Trans. Microwave Theory Tech., vol. 41, pp. 136–140, Jan. 1993.
[21] P. J. Soh, G. A. E. Vandenbosch, F. H. Wee, A. V. D. Bosch, M. Matrtinez-Vazquez and D. Schreurs, "Specific absorption rate (SAR) evaluation of textile antenna", *IEEE Antenna and Propagation Magazine*, vol. 57, no. 2, April 2015.
[22] T. Kawamura, K. Saito, S. Kikuchi, M. Takahashi, K. Ito, "Specific absorption rate measurement of birdcage coil for 3.0-T magnetic resonance imaging system employing thermographic method", IEEE tans on Microwave Theory and Techniques, vol. 57, no. 10, pp. 2508-2514, October 2009